Electronic Supplementary Material (ESI) for Environmental Science: Processes & Impacts.

Electronic supplementary information

As(V) in Magnetite: Incorporation and Redistribution

Brittany L. Huhmann[1,2#], Anke Neumann[3#], Maxim I. Boyanov[4,5], Kenneth M. Kemner[4], and Michelle M. Scherer[1]*

[1]Department of Civil and Environmental Engineering, University of Iowa, Iowa City, IA, 52242, United States

[2]*Present Address:* Department of Civil and Environmental Engineering, Massachusetts Institute of Technology, Cambridge, MA, 02139, United States

[3]School of Engineering, Newcastle University, Newcastle upon Tyne, NE1 7RU, United Kingdom

[4]Biosciences Division, Argonne National Laboratory, Argonne, IL, 60439, United States

[5]*Institute of Chemical Engineering, Bulgarian Academy of Sciences, Sofia 1113, Bulgaria*

[#]*Author Contributions*: Brittany Huhmann and Anke Neumann contributed equally to this work.

[*]*Corresponding Author*: phone: +44 191 208 6406; email: anke.neumann@ncl.ac.uk

This document contains:
Text on the Calculation of the extent of Fe atom exchange
5 Tables
11 Figures

Methods

Calculation of the extent of Fe atom exchange

The Fe isotope composition was analyzed on the ICP-MS as described previously[1-4] and is reported as Fe isotope fraction for isotope *i*:

$$f^i\mathrm{Fe} = \frac{^i\mathrm{counts}}{^{54}\mathrm{counts} + ^{56}\mathrm{counts} + ^{57}\mathrm{counts} + ^{58}\mathrm{counts}} \quad \text{(eq 1)}$$

To quantify the extent of Fe atom exchange between magnetite and aqueous Fe(II), we used the mass balance approach as previously described:[3,5]

$$Percent\ Magnetite\ Fe\ Exchange = \frac{N_{Fe(II)_{aq}} \times (f^iFe(II)^{ini}_{aq} - f^iFe(II)^{t}_{aq})}{N^{tot}_{Mag} \times (f^iFe(II)^{t}_{aq} - f^iFe^{ini}_{Mag})} \times 100 \quad \text{(eq 2)}$$

Here, $f^iFe(II)^{ini}_{aq}$, $f^iFe(II)^{t}_{aq}$, and $f^iFe^{ini}_{Mag}$ are the initial fraction of isotope *i* in aqueous Fe(II), the fraction of isotope *i* in aqueous Fe(II) at time t, and the initial fraction of isotope *i* in magnetite, respectively. $N_{Fe(II)_{aq}}$ and N^{tot}_{Mag} are the moles of Fe(II) added to solution and the moles of Fe in magnetite in the system. The "system" refers to the components that have participated in exchange and are at equilibrium after mixing.[3]

Table S1. Properties of magnetite used in this study (± 1 standard deviation, when given).

	Synthesis Parameters				Solid properties			
Sample ID	As:Fe mole ratio	pH	Temp. (°C)	Aging Time (day)	As:Fe mole ratio[a]	BET Surface area (m^2/g)	Stoichiometry (x[b])	Identity Confirmed by XRD?
Magnetite	0	10-11	Room temp.	1	n.m.[c]	65.30	0.45 ± 0.02[d]	Y
As(V)-Magnetite Coprecipitate	0.0011	10-11	Room temp.	1	0.0005 ± 0.00001[e]	n.m.	0.49 ± 0.04[d]	N
As(V)-Magnetite Coprecipitate	0.0070	10-11	Room temp.	1	n.m.	n.m.	n.m.	Y
As(V)-Magnetite Coprecipitate	0.0100	10-11	Room temp.	1	0.0099 ± 0.00153[d]	n.m.	0.50 ± 0.03[d]	Y

[a] As:Fe mole ratio determined by dissolution in HCl. As(V) concentration was measured on ICP-MS and Fe concentration was measured spectrophotometrically by the phenanthroline method.

[b] Magnetite Fe(II) content as defined by $x = \frac{{}^{Oct}Fe(II)}{{}^{Oct}Fe(III)+{}^{Tet}Fe(III)}$

[c] Not measured.

[d] Mean and one standard deviation of triplicate reactors of 15 mg magnetite dissolved in 5 M HCl.

[e] Mean and one standard deviation of triplicate reactors of 10 mg magnetite dissolved in 5 M HCl.

Table S2. Particle sizes.

	Diameter (nm)
Magnetite	11.3 (3.6)
Magnetite + 100 µM adsorbed As(V) + Fe(II), 7 d	9.3 (3)
As(V)-Magnetite Coprecipitate (0.0099)	8.7 (2.4)

Table S3. NaOH extractions of As(V) from magnetite following adsorption and coprecipitation, in the presence and absence of aqueous Fe(II).

		Initial added	Final Aqueous		NaOH extraction *"adsorbed"*		Residual solids *"incorporated"*		Total recovery	
		nmol	nmol	%	nmol	%	nmol	%	nmol	%
As(V) Coprecipitates										
As:Fe mole ratio = 0.0005	Adsorption Control	98	0(0)	0(0)	95(11)	97(11)	3(1)	4(1)	98(12)	100(12)
	Coprecipitate	64	---	---	18(2)	29(3)	44(5)	68(9)	64(7)	99(12)
As:Fe mole ratio = 0.0099	Adsorption Control	1912	31(28)	2(1)	1778(39)	93(1)	100(2)	5(0)	1909(12)	100(1)
	Coprecipitate	2055	---	---	524(116)	26(6)	1318(253)	64(12)	1842(368)	90(18)
	t = 32 d	2055	1(0)	0(0)	344(44)	17(2)	1472(260)	72(13)	1816 (303)	88(15)
	Coprecipitate + Fe(II)									
	t = 5 d	2055	0(0)	0(0)	538(63)	26(3)	1375(67)	67(3)	1914(88)	96(5)
	t = 32 d	2055	0(0)	0(0)	308(30)	15(1)	1540(150)	75(8)	1847(189)	90(9)
	t = 123 d	2055	0(0)	0(0)	352(75)	17(4)	1155(214)	56(10)	1507(279)	73(14)
Adsorbed As(V)										
As(V) concentration = 13.3 µM	Adsorbed As(V)									
	t = 2 d	200	8(15)	4(7)	165(12)	83(6)	5(1)	3(0)	182(2)	91(1)
	t = 34 d	200	0(0)	0(0)	168(8)	84(4)	13(1)	7(0)	182(8)	91(4)
	t = 124 d	200	0(0)	0(0)	156(3)	78(1)	25(1)	13(1)	182(3)	91(1)
	Adsorbed As(V) + Fe(II)									
	t = 2 d	200	0(0)	0(0)	165(5)	83(2)	7(1)	4(1)	179(4)	89(2)
	t = 18 d	200	0(0)	0(0)	146(7)	73(4)	27(4)	14(2)	173(11)	87(6)
	t = 34 d	200	0(0)	0(0)	160(6)	80(3)	28(15)	14(7)	187(20)	94(10)
	t = 124 d	200	0(0)	0(0)	139(3)	69(1)	31(1)	15(1)	170(3)	85(2)

Table S4. NaOH extractions of As(V) from magnetite following adsorption under experimental conditions identical to sample preparation for XAS analysis. Experimental conditions: 10 g L^{-1} magnetite, 1 mM Fe(II), in 15 mL 50 mM MOPS at pH 7.2

		Initial added	Final Aqueous		NaOH extraction *"adsorbed"*		Residual solids *"incorporated"*		Total recovery	
		nmol	nmol	%	nmol	%	nmol	%	nmol	%
	Adsorbed As(V) + Fe(II)									
As(V) concentration = 2933 µM	t = 0 d (30 min, no Fe(II) present)	46,387	13,601 (267)	29 (1)	31,584 (638)	68 (1)	724 (26)	2 (0)	45,909 (931)	99 (2)
	t = 1 d	46,264	64 (27)	0 (0)	44,117 (952)	95 (2)	882 (15)	2 (0)	45,036 (994)	97 (2)
	t = 7.65 d	47,073	2 (0)	0 (0)	41,865 (1,176)	89 (2)	1,604 (33)	3 (0)	43,472 (1,209)	92 (3)

Table S5. Extent of Fe(II)-catalyzed Fe atom exchange in magnetite, magnetite with sorbed As(V) and As(V)-coprecipitated magnetite. Experiments were conducted with 1 gL^{-1} magnetite in 50 mM MOPS at pH 7.2.

		Aqueous Fe(II)					**Residual Solid**					TOTAL	
	Time (day)	Fe(II) (µmol)	% ^{57}Fe	% ^{54}Fe	% Ex. (^{57}Fe)	% Ex. (^{54}Fe)	Fe (µmol)	% ^{57}Fe	% ^{54}Fe	% Ex. (^{57}Fe)	% Ex. (^{54}Fe)	% Fe Recovery	pH
No As(V)	0	14.5 (0.2)	90.4 (1)	0.5 (0.1)	0 (0.1)	0 (0.1)	213 (23)	2.4 (0.1)	5.1 (0.1)	0 (0.1)	0 (1.2)	109 (11)	---
	0.01	14.5 (0.3)	62.6 (11.3)	1.9 (0.6)	3.9 (2.4)	3.4 (2.2)	184 (54)	4.6 (0.4)	4.9 (0.1)	4 (1.6)	5.8 (4.2)	95 (26)	7.27 (0.03)
	4.78	12.7 (0.4)	40.3 (5.3)	3 (0.2)	10.5 (2.4)	9.2 (1.8)	204 (31)	6.6 (0.2)	4.7 (0.1)	11.4 (1.5)	16.6 (5.8)	104 (15)	7.15 (0.05)
	6.91	12.7 (1.5)	42.7 (5.5)	2.9 (0.3)	9.4 (2.5)	8.6 (2.5)	228 (27)	6.5 (0.3)	4.7 (0)	10.6 (2.3)	15.6 (2.4)	115 (12)	7.16 (0.04)
As(V) Ads 13.3 µM	0	14.2 (0.4)	82.7 (1.9)	1.1 (0.07)	0 (0.2)	0 (0.1)	213 (23)	2.4 (0.1)	5.1 (0.1)	0 (0.1)	0 (1.4)	109 (11)	---
	0.01	19.6 (2.9)	46.9 (6.8)	2.8 (0.3)	6.5 (2.4)	5.8 (1.9)	178 (3)	4.6 (0.2)	5.1 (0.1)	5.2 (0.4)	-0.8 (3.5)	94 (1)	7.14 (0.11)
	4.77	15.3 (0.5)	40.2 (2.2)	3.1 (0.1)	8.7 (1)	8.3 (0.8)	187 (2)	6.3 (0.4)	4.8 (0.2)	10.3 (1.2)	12.1 (8.7)	97 (1)	7.17 (0.02)
	6.91	14.8 (0.3)	37.1 (1.7)	3.3 (0.1)	10.2 (0.9)	9.9 (0.6)	183 (9)	6.9 (0)	4.9 (0)	13 (0.6)	8 (2.2)	95 (4)	7.17 (0.05)
As(V) Ads 100 µM	0	14.6 (0.4)	90.8 (1)	0.3 (0)	0 (0.1)	0 (0.1)	213 (23)	5.1 (0.1)	5.1 (0.1)	2.6 (0)	0 (1.2)	109 (11)	---
	0.01	14.5 (0.3)	67 (3)	1.6 (0.2)	2.9 (0.6)	2.9 (0.6)	194 (12)	3.9 (0)	4.8 (0.1)	5.9 (0.3)	7.7 (2.3)	100 (6)	7.25 (0.01)
	4.77	14.2 (0.3)	47.2 (6.5)	2.6 (0.4)	7.8 (2.3)	7.1 (2.6)	187 (8)	5.6 (0.1)	4.7 (0)	12.1 (1.6)	14.4 (2.4)	97 (4)	7.17 (0.01)
	6.95	13.4 (0.5)	46.2 (5.7)	2.6 (0.3)	8 (2.2)	7.2 (1.9)	185 (30)	5.4 (0.2)	4.7 (0)	11.9 (2)	14.8 (2.2)	95 (15)	7.18 (0.02)
As(V) Ads 200 µM	0	17 (1.6)	87.3 (2)	0.5 (0.1)	0 (0.2)	0 (0.1)	213 (23)	5.1 (0.1)	5.1 (0.1)	2.7 (0.1)	0 (1.3)	110 (12)	---
	0.01	14.2 (0.1)	70 (3.9)	1.5 (0.2)	2.1 (0.6)	2 (0.5)	210 (9)	3.7 (0.1)	4.7 (0)	5.3 (0.3)	8.9 (0.6)	107 (4)	7.17 (0.01)
	5.04	13 (0.2)	60.6 (1.6)	1.9 (0.1)	3.6 (0.3)	3.5 (0.5)	177 (11)	5.2 (0.4)	4.7 (0)	8.5 (0.9)	12.1 (0.8)	91 (5)	7.14 (0.02)
	6.82	12.6 (0.2)	57.4 (3.1)	2.1 (0.2)	4.2 (0.7)	4.1 (0.7)	191 (14)	5.3 (0.1)	4.7 (0)	9.2 (0.6)	12.6 (1.5)	98 (7)	7.16 (0.02)
As(V) Coppt As:Fe = 0.0005	0	15.6 (0.2)	76 (7.1)	1.2 (0.34)	0 (0.8)	0 (0.7)	190 (16)	2.4 (0)	4.9 (0.0)	0 (0)	0 (0.3)	98 (8)	---
	0.01	18.7 (0.4)	32.1	3.4	11.4	11.2	1967 (16)	6.6 (0.2)	4.7 (0.0)	14.6 (1.1)	13.9 (3.3)	103 (7)	7.16 (0.02)
	5.33	12.6 (0.6)	27.1 (2.4)	3.6 (0.12)	15.4 (2.3)	15 (2.2)	189 (2)	8.7 (0.6)	4.6 (0.0)	26 (3.4)	24.4 (1.4)	96 (1)	7.14 (0.03)
	7.82	13.1 (0.5)	28.8 (2.7)	3.6 (0.14)	13.9 (2.1)	13.7 (2.2)	177 (3)	9 (0.1)	4.6 (0.1)	25.3 (2.1)	26.1 (5.9)	91 (1)	7.10 (0.01)
As(V) Coppt As:Fe = 0.0099	0	15.8 (0.2)	94.1 (1.1)	0.2 (0.1)	0 (0.1)	0 (0.1)	183 (41)	4.8 (0)	0 (0)	0 (0)	0 (0.6)	95 (20)	---
	0.01	13.5 (0.9)	75.3 (2.2)	1.2 (0.1)	2 (0.3)	2.1 (0.3)	183 (15)	4.8 (0.1)	3.7 (0.1)	3.7 (0.1)	3.6 (0.9)	94 (7)	7.16 (0.03)
	5.07	5.3 (0.3)	30 (2.8)	3.5 (0.2)	17.9 (2.6)	19.2 (3.2)	183 (32)	9 (0.5)	24.7 (0.8)	24.7 (0.8)	24.7 (2.9)	90 (15)	7.04 (0.01)
	6.97	5.1 (0.2)	32.1 (5.5)	3.4 (0.3)	16.6 (4.6)	17.2 (4.8)	166 (32)	9.7 (0.9)	25.4 (1.8)	25.4 (1.8)	24.2 (3.4)	82 (15)	7.03 (0.01)

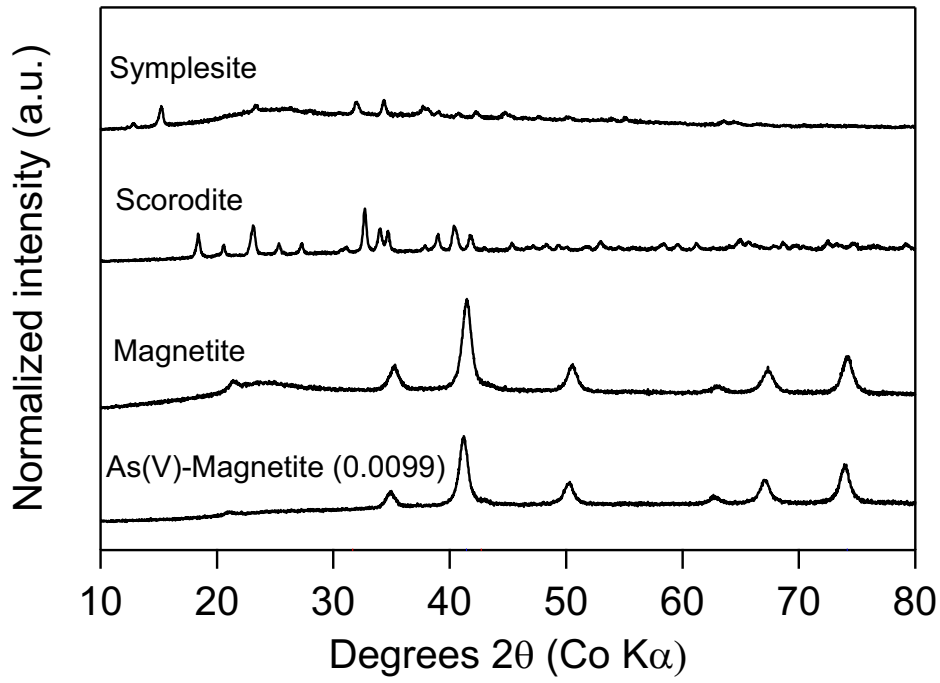

Figure S1. Powder X-ray diffraction pattern of the magnetite and As(V)-magnetite coprecipitate used in this study as compared with patterns for symplesite ($Fe^{II}_3(AsO_4)_2 \bullet 8(H_2O)$) and scorodite ($Fe^{III}AsO_4 \bullet 2(H_2O)$).

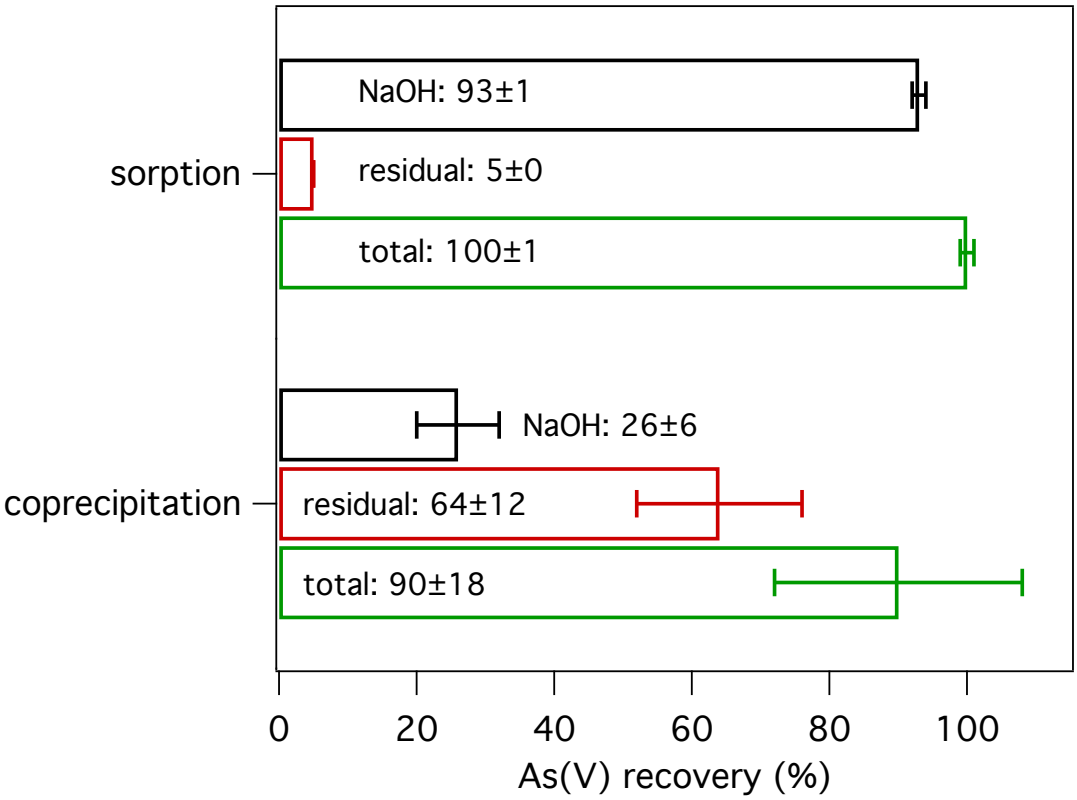

Figure S2. As recovered from magnetite with sorbed As(V) and As(V)-magnetite coprecipitates in the NaOH extraction step and subsequent total dissolution. In both experiments, the molar As:Fe ratio was 0.0099 and the overall total As recovery was ≥90%.

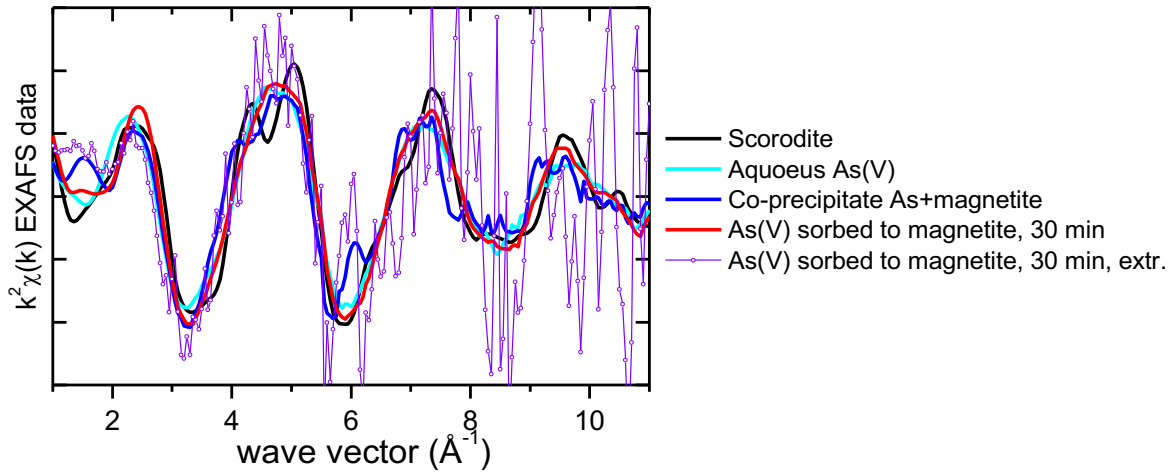

Figure S3. As K-edge EXAFS data of As(V) sorbed to magnetite for 30 min before (red line) and after (purple symbols) extraction with NaOH. The small fraction of As(V) remaining on the NaOH-extracted solids is responsible for the low signal-to-noise ratio of the measured spectrum, which impairs further structural analysis. Qualitative comparisons in the lower-noise region at low *k* suggests similarity to the co-precipitate sample (blue line), particularly around 1.8 $Å^{-1}$ and 6 $Å^{-1}$.

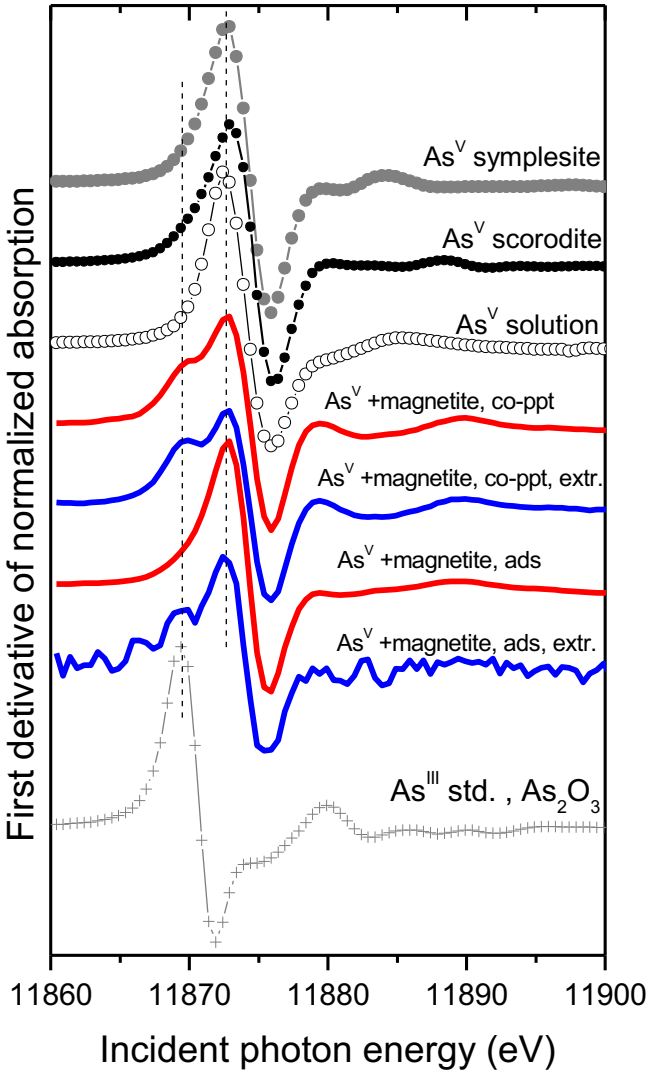

Figure S4. First derivative of the normalized absorption spectra from samples and standards. Magnetite with sorbed As(V) and As(V)-magnetite coprecipitate (As:Fe mole ratio of 0.007) samples are shown before and after extraction with NaOH. The vertical dashed lines indicate spectral features that correspond to the As(III) and As(V) standards.

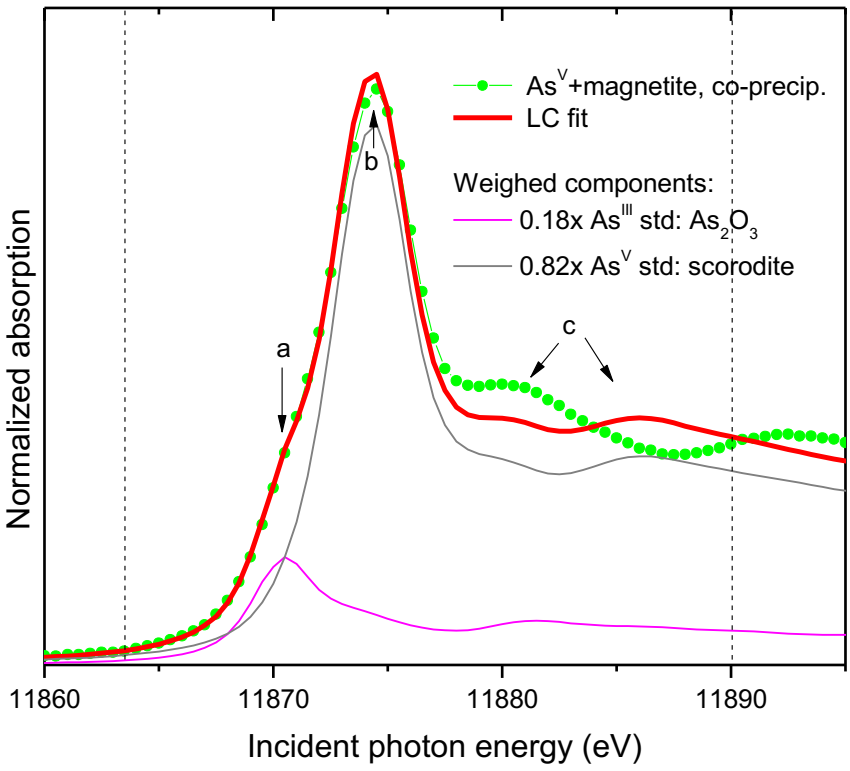

Figure S5. Linear combination (LC) fit of the XANES data from the As(V)-magnetite co-precipitation sample with As(III) and As(V) standards (data: green symbols, fit: red line). The fit range is shown by the dashed lines. The weighted contributions in the LC fit from the As(III) standard (magenta), and the As(V) standard (grey) are shown. The ~18% contribution from the As(III) standard is able to reproduce the shoulder at the edge position (arrow a) and the white line amplitude suppression (arrow b). The inability of the LC fit to reproduce the features indicated by arrow c is due to the different atomic coordination of As in the co-precipitation sample relative to the scorodite standard used here as a valence state reference.

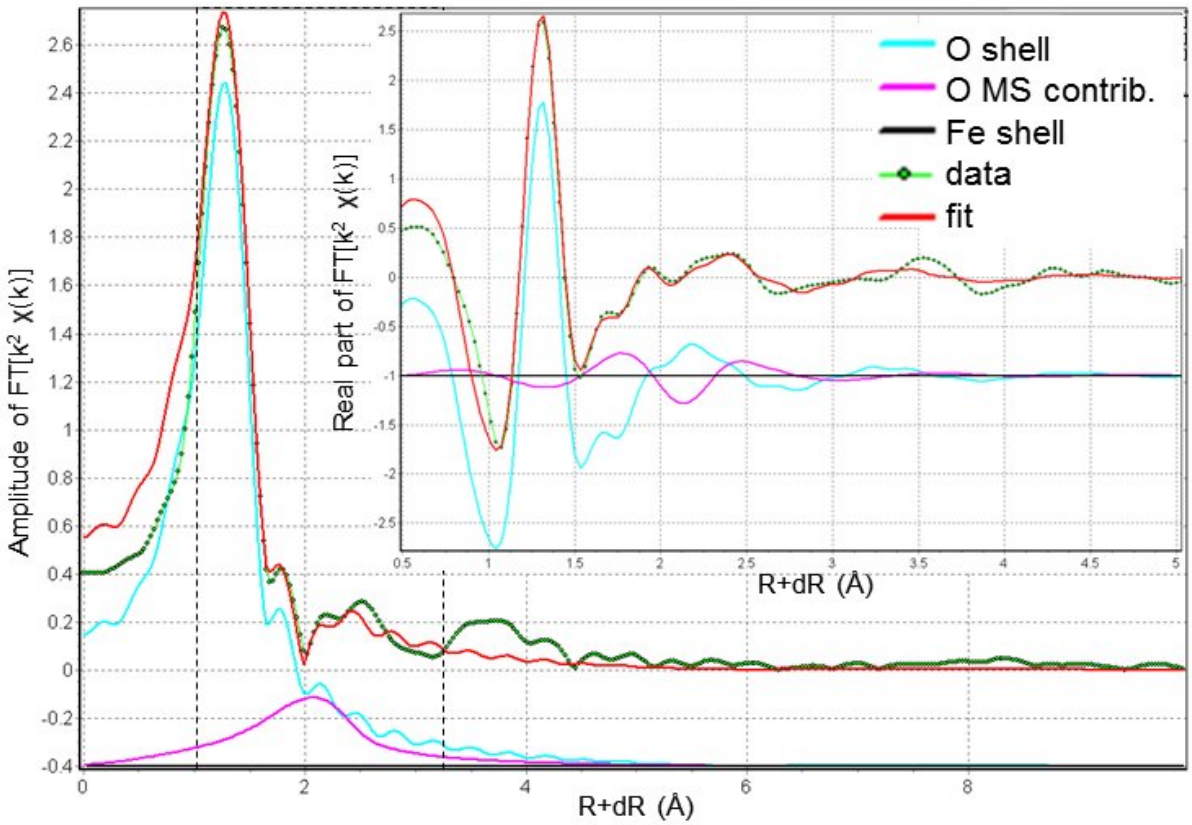

Figure S6a. Illustration of the fit quality for the EXAFS data from the aqueous As(V) standard. Main figure: magnitude of the Fourier Transform (FT), inset: real part of FT. The FT is over Δk = 2.8 - 12.1 $Å^{-1}$ with 1.0 $Å^{-1}$ wide Hanning window sills. The data are in green symbols, the fit is the red lines. The fit range is shown by the dotted lines. The contribution from the O shell (cyan) and the MS contribution within the AsO_4 tetrahedron (magenta) are also shown. Note that the individual contributions combine linearly to produce the fit line only in the real part of the FT. The numerical values and the constraints used in the fit are listed in Table 2.

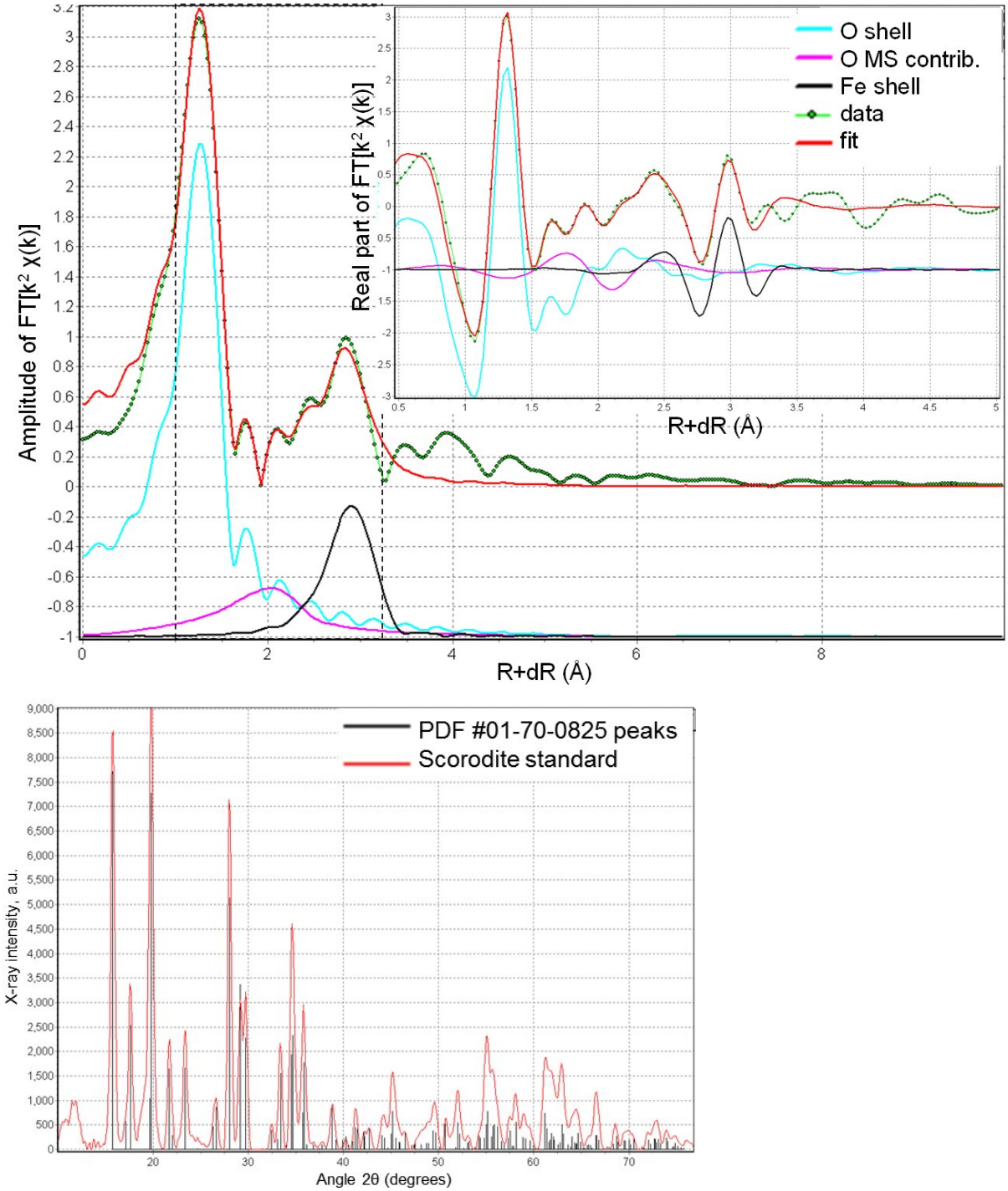

Figure S6b. Illustration of the fit for the EXAFS data from the scorodite standard. Main figure: magnitude of the Fourier Transform (FT), inset: real part of FT. The FT is over $\Delta k = 2.8 = 12.1$ Å^{-1} with 1.0 Å^{-1} wide Hanning window sills. The data are in green symbols, the fit is the red lines. The fit range is shown by the dotted line. The numerical values and the constraints used in the fit are listed in Table 2. The powder XRD pattern verifying that the standard is scorodite is shown at the bottom.

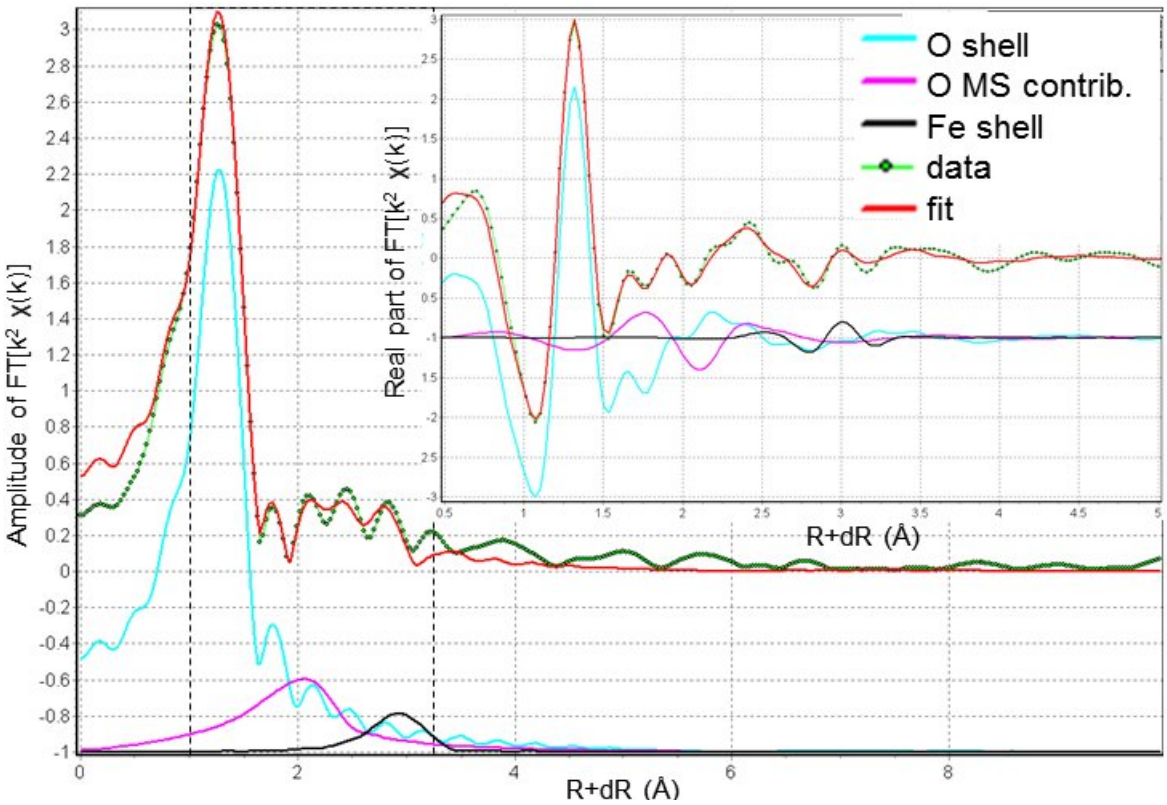

Figure S6c. Illustration of the fit quality for the EXAFS data from the As(V) + magnetite, adsorption, 30 min sample. Main figure: magnitude of the Fourier Transform (FT), inset: real part of FT. The FT is over Δk = 2.8 - 12.1 $Å^{-1}$ with 1.0 $Å^{-1}$ wide Hanning window sills. The data are in green symbols, the fit is the red lines. The fit range is shown by the dotted lines. The individual contributions from the O shell (cyan), the MS paths within the AsO_4 tetrahedron (magenta), and the Fe shell (black) are also shown. The numerical values and the constraints used in the fit are listed in Table 2.

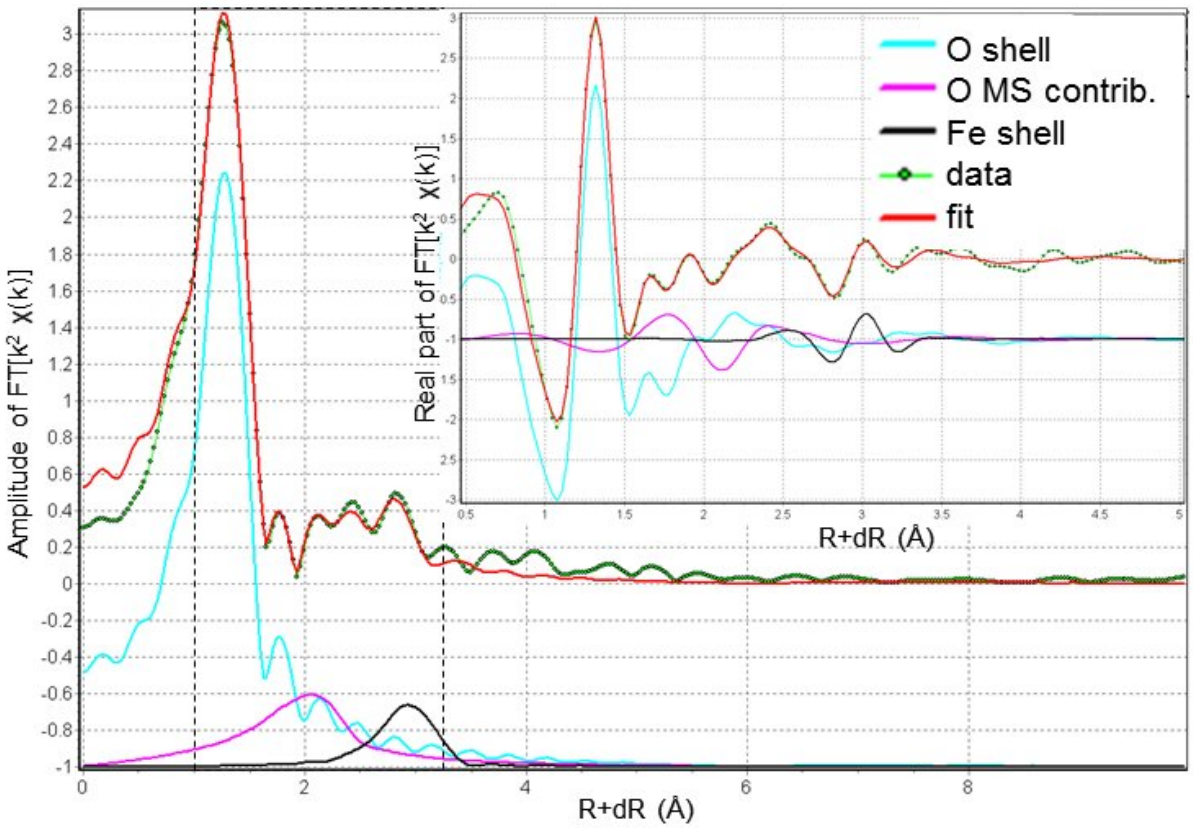

Figure S6d. Illustration of the fit quality for the EXAFS data from the As(V) + magnetite, adsorption, 3.5 d sample. Main figure: magnitude of the Fourier Transform (FT), inset: real part of FT. The FT is over $\Delta k = 2.8 - 12.1$ Å^{-1} with 1.0 Å-1 wide Hanning window sills. The data are in green symbols, the fit is the red lines. The fit range is shown by the dotted lines. The individual contributions from the O shell (cyan), the MS paths within the AsO_4 tetrahedron (magenta), and the Fe shell (black) are also shown. The numerical values and the constraints used in the fit are listed in Table 2.

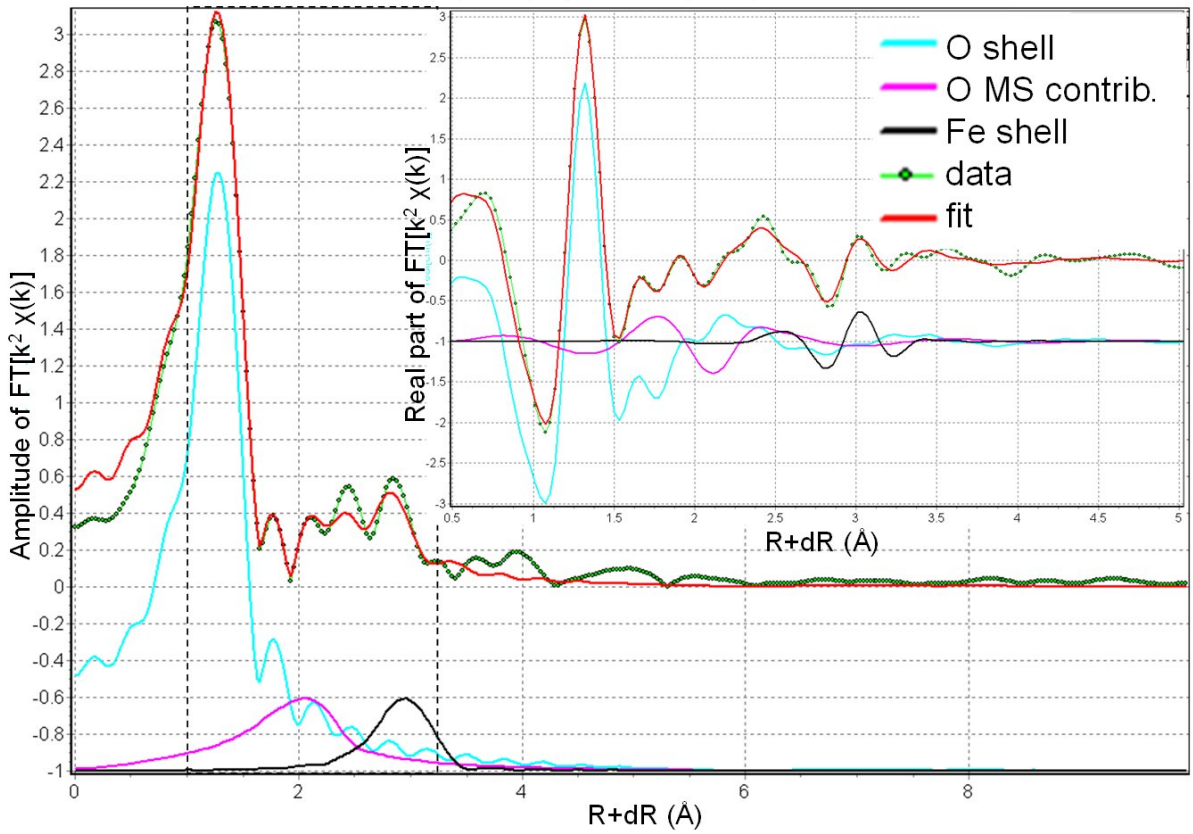

Figure S6e. Illustration of the fit quality for the EXAFS data from the As(V) + magnetite, adsorption, 4 weeks sample. Main figure: magnitude of the Fourier Transform (FT), inset: real part of FT. The FT is over Δk = 2.8 - 12.1 $Å^{-1}$ with 1.0 $Å^{-1}$ wide Hanning window sills. The data are in green symbols, the fit is the red lines. The fit range is shown by the dotted lines. The individual contributions from the O shell (cyan), the MS paths within the AsO_4 tetrahedron (magenta), and the Fe shell (black) are also shown. The numerical values and the constraints used in the fit are listed in Table 2.

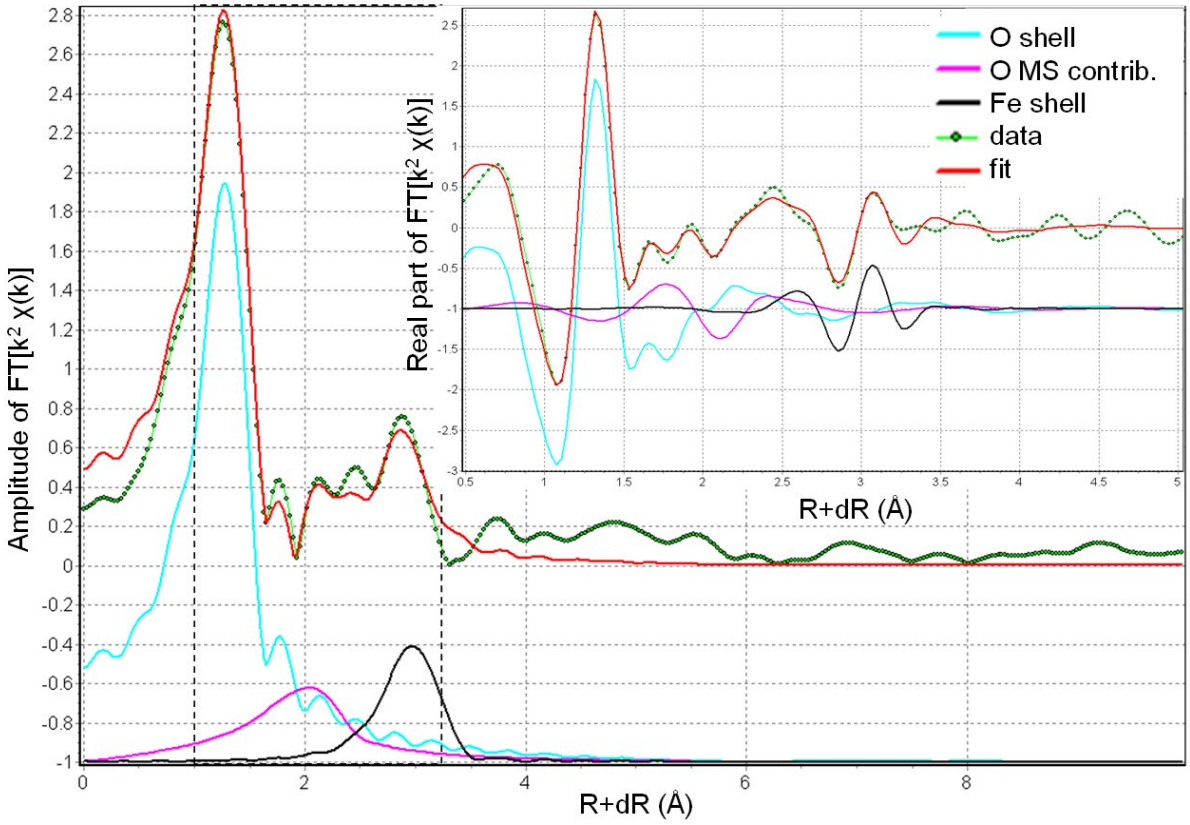

Figure S6f. Illustration of the fit quality for the EXAFS data from the As(V) + magnetite, co-precipitation sample. Main figure: magnitude of the Fourier Transform (FT), inset: real part of FT. The FT is over Δk = 2.8 - 12.1 $Å^{-1}$ with 1.0 $Å^{-1}$ wide Hanning window sills. The data are in green symbols, the fit is the red lines. The fit range is shown by the dotted lines. The individual contributions from the O shell (cyan), the MS paths within the AsO_4 tetrahedron (magenta), and the Fe shell (black) are also shown. The numerical values and the constraints used in the fit are listed in Table 2.

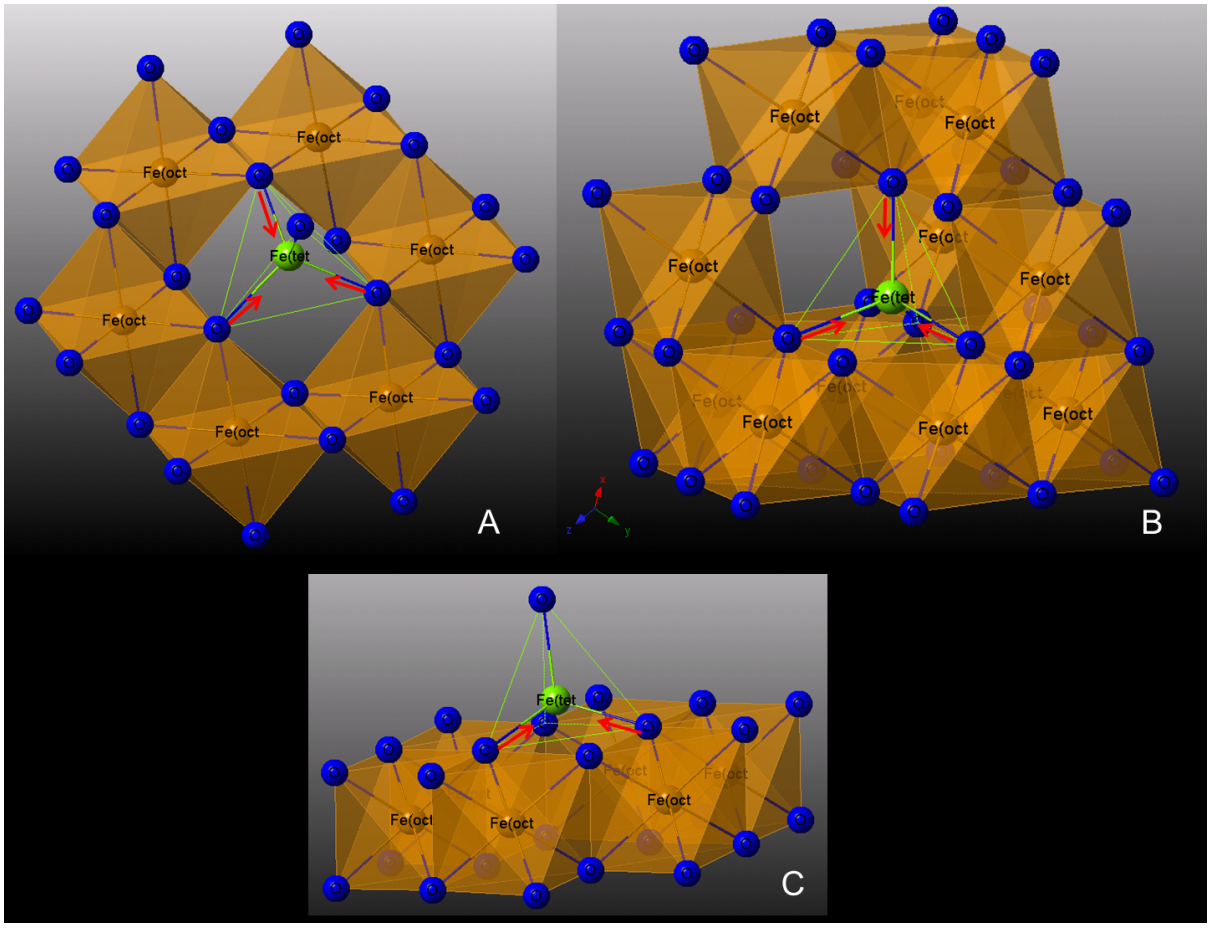

Figure S7. Arrangement of the Fe octahedra (orange) around the tetrahedral Fe site (green) in magnetite. Depiction based on the crystallographic data in Haavik et al. (reference 57 in the main text). The tetrahedral site occupies the space above the void in the octahedral (111) plane. The distortions required to fit the shorter-distance As(V) octahedron are show by red arrows. (A) View from above the (111) plane; (B) View along the (111) plane, with some octahedra above the plane shown; (C) View along the (111) plane, without additional Fe octahedral above the plane.

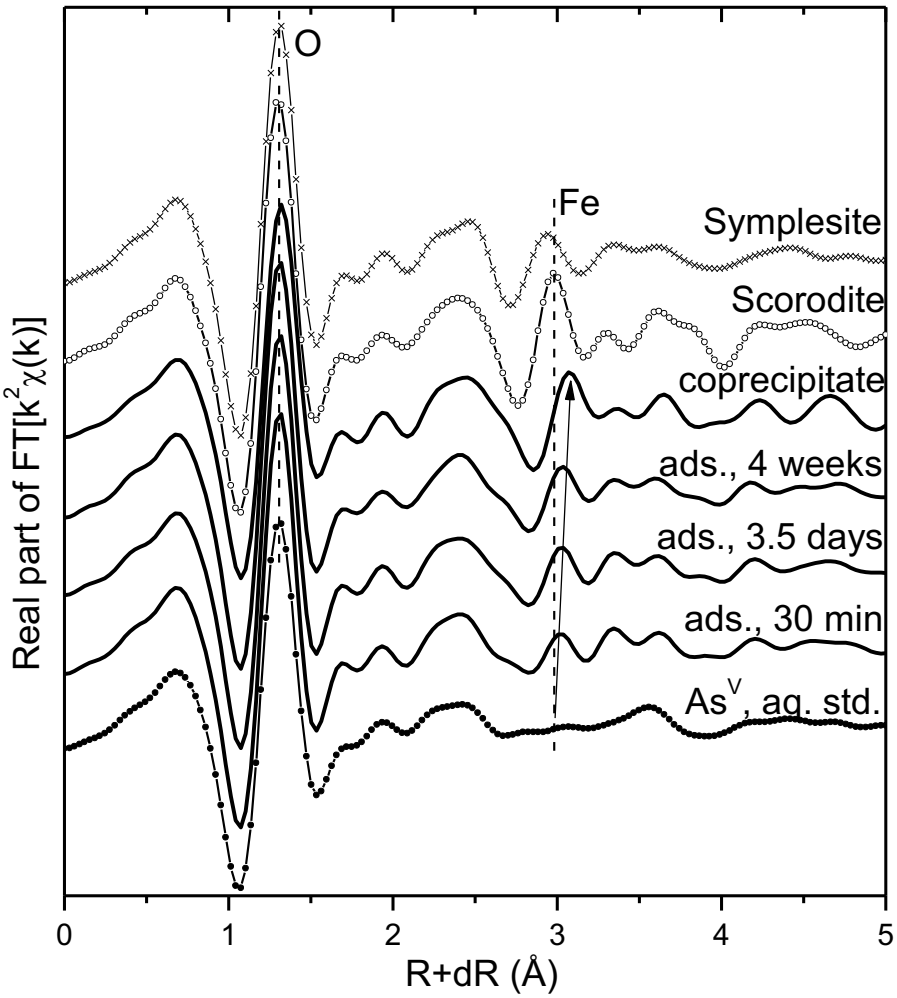

Figure S8. Fourier transform of the k^2-weighted As K-edge EXAFS data (real part) of sorbed As(V) and magnetite coprecipitated As(V) as well as As reference materials (aqueous As(V), Fe-As phases symplesite and scorodite). The vertical dashed lines indicate the features corresponding to the O and Fe coordination shells in scorodite. Experimental data presented as solid lines and standards as lines with symbols. The arrow indicates the increasing As-Fe distance in the sorption samples with reaction time.

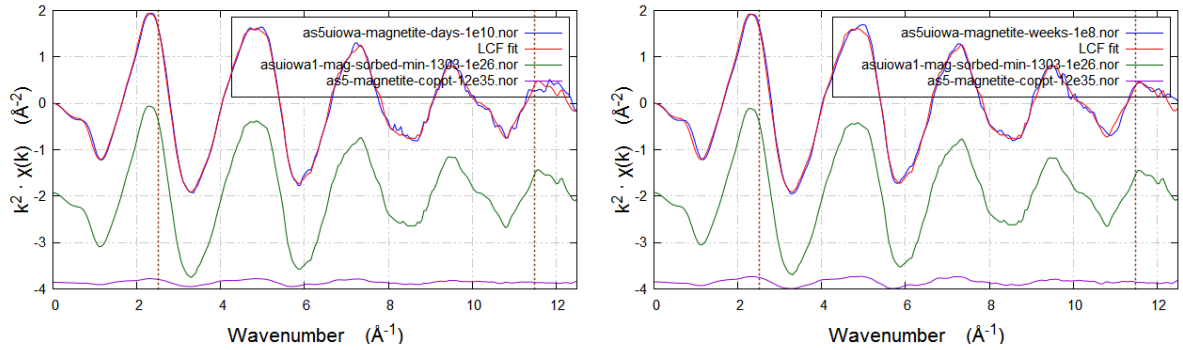

Figure S9. Linear combination (LC) fits of the EXAFS data from As(V) sorbed to magnetite after 3.5 d (left) and 28 d (right), using the adsorption and co-precipitation samples as endmembers. The data are shown in blue lines, the fit is shown in red lines. The fit range is indicated by the dotted lines. The weighted contributions in the LC fit from the 30 min adsorption sample (green), and the As(V)-magnetite co-precipitation sample (purple) are shown at the bottom. The refined proportions of the spectral endmembers are 5% co-precipitated standard for the 3.5 d sample and 8% co-precipitated standard for the 28 d sample, balance is the 30 min adsorption standard. These numerical values are discussed in the main text.

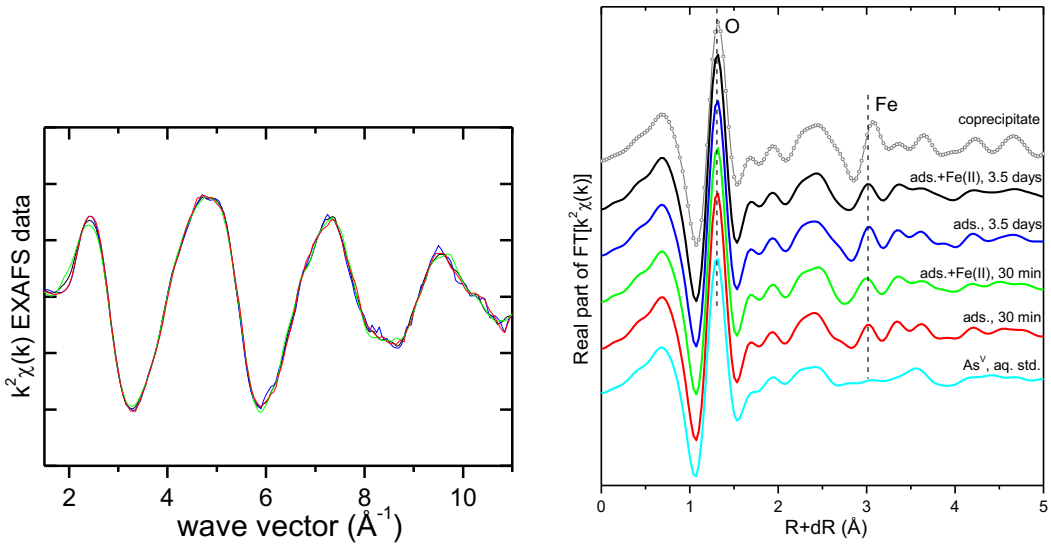

Figure S10: Left: Comparison of the k^2-weighted EXAFS spectra from As(V) adsorbed on magnetite with and without added Fe(II) for 30 min and 3.5 d, showing that the same data are obtained in all reactors. Right: Real part of the Fourier transformed EXAFS data from the left figure compared to the aqueous As(V) standard and As(V) co-precipitated with magnetite. The spectra are offset vertically for clarity. The same color convention is used in both graphs.

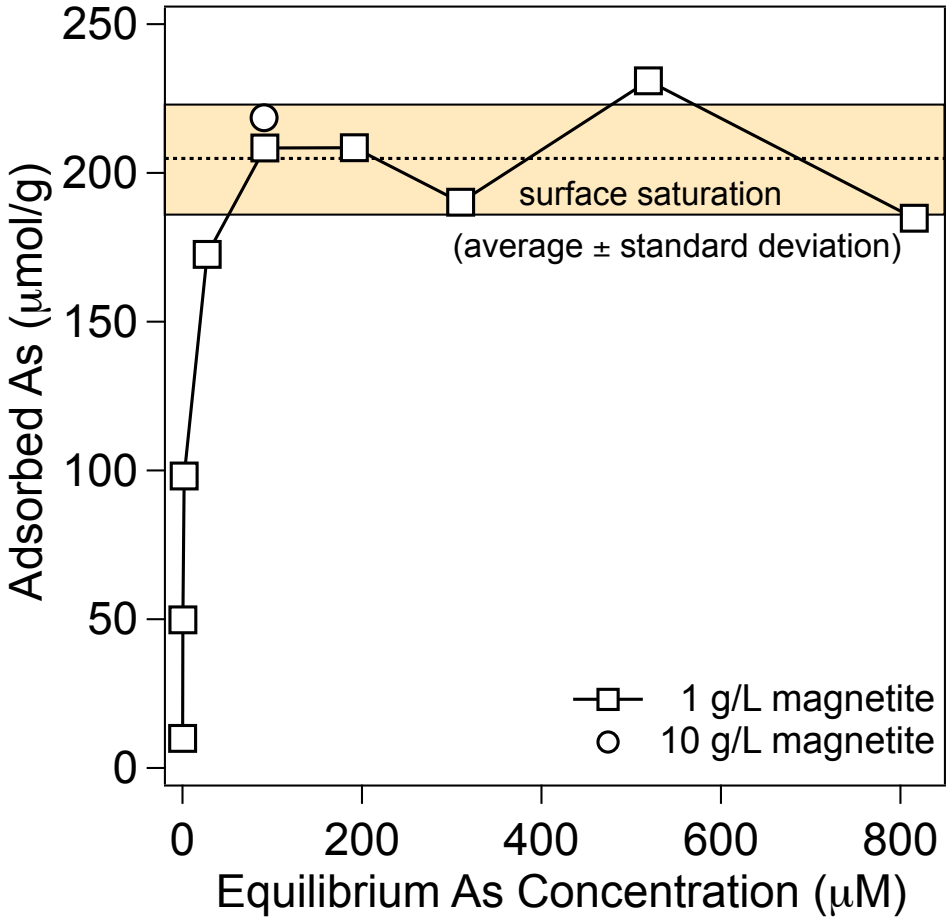

Figure S11. As(V) adsorption isotherm on magnetite (solids loading 1 g L^{-1}) buffered at pH 7.2 with 50 mM MOPS. Data from XAS reactors (10 g/L, 3092 μM initial As(V) concentration; from Table S4) was re-calculated to match the same solids loading by dividing the equilibrium aqueous As concentration by 10 (ratio of mass loadings).

References

1. Frierdich AJ, Helgeson M, Liu C, Wang C, Rosso KM, Scherer MM. Iron Atom Exchange between Hematite and Aqueous Fe(II). Environ Sci Technol. 2015;49(14):8479-86.
2. Gorski CA, Handler RM, Beard BL, Pasakarnis T, Johnson CM, Scherer MM. Fe Atom Exchange between Aqueous Fe^{2+} and Magnetite. Environ Sci Technol. 2012;46:12399-407.
3. Handler RM, Frierdich AJ, Johnson CM, Rosso KM, Beard BL, Wang C, Latta DE, Neumann A, Pasakarnis T, Premaratne WAPJ, Scherer MM. Fe(II)-Catalyzed Recrystallization of Goethite Revisited. Environ Sci Technol. 2014;48(19):11302-11.
4. Latta DE, Bachman JE, Scherer MM. Fe Electron Transfer and Atom Exchange in Goethite: Influence of Al-Substitution and Anion Sorption. 2012.
5. Mikutta C, Wiederhold JG, Cirpka OA, Hofstetter TB, Bourdon B, von Gunten U. Iron isotope fractionation and atom exchange during sorption of ferrous iron to mineral surfaces. Geochim Cosmochim Acta. 2009;73:1795-812.